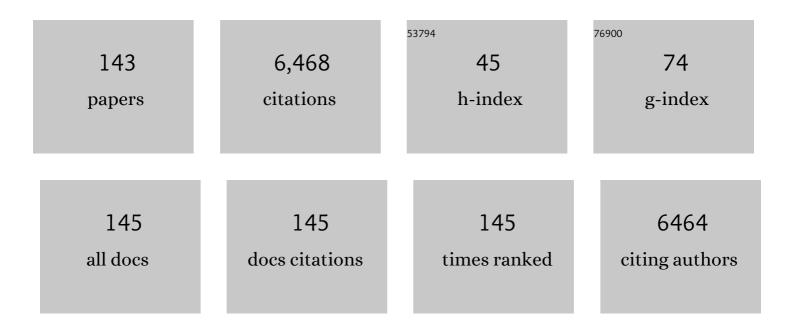
List of Publications by Year in descending order

Source: https://exaly.com/author-pdf/1668604/publications.pdf Version: 2024-02-01



#	Article	IF	CITATIONS
1	Metal–Support Interaction: Group VIII Metals and Reducible Oxides. Advances in Catalysis, 1989, 36, 173-235.	0.2	400
2	Recent advances in the selective catalytic reduction of NOx with NH3 on Cu-Chabazite catalysts. Applied Catalysis B: Environmental, 2017, 202, 346-354.	20.2	298
3	Coke formation and deactivation pathways on H-ZSM-5 in the conversion of methanol to olefins. Journal of Catalysis, 2015, 325, 48-59.	6.2	289
4	On reaction pathways in the conversion of methanol to hydrocarbons on HZSM-5. Journal of Catalysis, 2014, 317, 185-197.	6.2	236
5	A carbon nanotube–polymer composite for T-cell therapy. Nature Nanotechnology, 2014, 9, 639-647.	31.5	190
6	Metal-support effects in Pt/L-zeolite catalysts. Catalysis Letters, 1989, 3, 103-110.	2.6	145
7	Synthesis and Characterization of Highly Ordered Coâ^'MCM-41 for Production of Aligned Single Walled Carbon Nanotubes (SWNT). Journal of Physical Chemistry B, 2003, 107, 11048-11056.	2.6	145
8	Uniform-Diameter Single-Walled Carbon Nanotubes Catalytically Grown in Cobalt-Incorporated MCM-41. Journal of Physical Chemistry B, 2004, 108, 503-507.	2.6	138
9	Carbon nanotube-supported Pt-based bimetallic catalysts prepared by a microwave-assisted polyol reduction method and their catalytic applications in the selective hydrogenation. Journal of Catalysis, 2010, 276, 314-326.	6.2	136
10	On the impact of co-feeding aromatics and olefins for the methanol-to-olefins reaction on HZSM-5. Journal of Catalysis, 2014, 314, 21-31.	6.2	135
11	Synthesis and Characterization of Vanadium-Substituted Mesoporous Molecular Sieves. Journal of Physical Chemistry B, 1999, 103, 2113-2121.	2.6	111
12	The dynamics of CO oxidation on Pd, Rh, and Pt studied by highâ€resolution infrared chemiluminescence spectroscopy. Journal of Chemical Physics, 1991, 95, 6932-6944.	3.0	108
13	Synthesis of uniform diameter single-wall carbon nanotubes in Co-MCM-41: effects of the catalyst prereduction and nanotube growth temperatures. Journal of Catalysis, 2004, 225, 453-465.	6.2	105
14	Enhanced Cellular Activation with Single Walled Carbon Nanotube Bundles Presenting Antibody Stimuli. Nano Letters, 2008, 8, 2070-2076.	9.1	104
15	Chiral-Selective CoSO ₄ /SiO ₂ Catalyst for (9,8) Single-Walled Carbon Nanotube Growth. ACS Nano, 2013, 7, 614-626.	14.6	101
16	Effect of surface oxygen containing groups on the catalytic activity of multi-walled carbon nanotube supported Pt catalyst. Applied Catalysis B: Environmental, 2010, 101, 21-30.	20.2	93
17	Synthesis and Characterization of Highly Ordered Ni-MCM-41 Mesoporous Molecular Sieves. Journal of Physical Chemistry B, 2005, 109, 13237-13246.	2.6	90
18	New catalytic concepts from new materials: understanding catalysis from a fundamental perspective, past, present, and future. Journal of Catalysis, 2003, 216, 12-22.	6.2	85

#	Article	IF	CITATIONS
19	Role of the ionic environment in enhancing the activity of reacting molecules in zeolite pores. Science, 2021, 372, 952-957.	12.6	79
20	Selective Synthesis of Subnanometer Diameter Semiconducting Single-Walled Carbon Nanotubes. Journal of the American Chemical Society, 2010, 132, 11125-11131.	13.7	78
21	Synthesis, Characterization, and Stability of Feâ^'MCM-41 for Production of Carbon Nanotubes by Acetylene Pyrolysis. Journal of Physical Chemistry B, 2005, 109, 2645-2656.	2.6	77
22	Electronic effects and effects of particle morphology in n-hexane conversion over zeolite-supported platinum catalysts. Journal of Catalysis, 1998, 177, 175-188.	6.2	75
23	Gas phase methanol oxidation on V-MCM-41. Applied Catalysis A: General, 1999, 188, 277-286.	4.3	75
24	(n,m) Abundance Evaluation of Single-Walled Carbon Nanotubes by Fluorescence and Absorption Spectroscopy. Journal of the American Chemical Society, 2006, 128, 15511-15516.	13.7	75
25	Single-Atom Pt Catalyst for Effective C–F Bond Activation via Hydrodefluorination. ACS Catalysis, 2018, 8, 9353-9358.	11.2	70
26	The Adsorption and Reaction of Coordination Complexes on Silica Gel. Inorganic Chemistry, 1965, 4, 1123-1128.	4.0	66
27	Synthesis of uniform diameter single wall carbon nanotubes inBCo-MCM-41: effects of CO pressure and reaction time. Journal of Catalysis, 2004, 226, 351-362.	6.2	66
28	Diameter Tuning of Single-Walled Carbon Nanotubes with Reaction Temperature Using a Co Monometallic Catalyst. Journal of Physical Chemistry C, 2009, 113, 10070-10078.	3.1	65
29	The effect of the cobalt loading on the growth of single wall carbon nanotubes by CO disproportionation on Co-MCM-41 catalysts. Carbon, 2006, 44, 67-78.	10.3	64
30	Pt–Co bimetallic catalyst supported on single walled carbon nanotube: XAS and aqueous phase reforming activity studies. Catalysis Today, 2009, 146, 160-165.	4.4	62
31	Synthesis, Characterization, and Catalytic Performance of Highly Dispersed Co-SBA-15. Journal of Physical Chemistry C, 2009, 113, 14863-14871.	3.1	60
32	<i>In Situ</i> Identification of Reaction Intermediates and Mechanistic Understandings of Methane Oxidation over Hematite: A Combined Experimental and Theoretical Study. Journal of the American Chemical Society, 2020, 142, 17119-17130.	13.7	59
33	Preparation of Highly Ordered Vanadium-Substituted MCM-41: Stability and Acidic Propertiesâ€. Journal of Physical Chemistry B, 2002, 106, 8437-8448.	2.6	57
34	Mechanism of Cobalt Cluster Size Control in Co-MCM-41 during Single-Wall Carbon Nanotubes Synthesis by CO Disproportionation. Journal of Physical Chemistry B, 2004, 108, 15565-15571.	2.6	57
35	Low-Defect, Purified, Narrowly (n,m)-Dispersed Single-Walled Carbon Nanotubes Grown from Cobalt-Incorporated MCM-41. ACS Nano, 2007, 1, 327-336.	14.6	56
36	Catalytic performance of vanadium incorporated MCM-41 catalysts for the partial oxidation of methane to formaldehyde. Applied Catalysis A: General, 2006, 302, 48-61.	4.3	55

#	Article	IF	CITATIONS
37	Catalytic behavior of vanadium substituted mesoporous molecular sieves. Catalysis Today, 1999, 51, 501-511.	4.4	54
38	Controlling Hydrodeoxygenation of Stearic Acid to <i>n</i> â€Heptadecane and <i>n</i> â€Octadecane by Adjusting the Chemical Properties of Ni/SiO ₂ –ZrO ₂ Catalyst. ChemCatChem, 2017, 9, 195-203.	3.7	53
39	Role of Surface Cobalt Silicate in Single-Walled Carbon Nanotube Synthesis from Silica-Supported Cobalt Catalysts. ACS Nano, 2010, 4, 1759-1767.	14.6	49
40	Surface and Bulk Characterisation of Metallic Phases Present during CO Hydrogenation over Pd–Cu/KL Zeolite Catalysts. Journal of Catalysis, 1996, 164, 477-483.	6.2	48
41	Evidence for anchoring and partial occlusion of metallic clusters on the pore walls of MCM-41 and effect on the stability of the metallic clusters. Catalysis Today, 2007, 123, 122-132.	4.4	48
42	Clustering of Stimuli on Single-Walled Carbon Nanotube Bundles Enhances Cellular Activation. Langmuir, 2010, 26, 5645-5654.	3.5	48
43	Effect of Manganese Addition to the Co-MCM-41 Catalyst in the Selective Synthesis of Single Wall Carbon Nanotubes. Journal of Physical Chemistry C, 2009, 113, 21611-21620.	3.1	47
44	Impurity effects in the interaction of oxygen with Rh(111). Applications of Surface Science, 1982, 10, 546-558.	1.0	46
45	Enhancement of Dehydrogenation and Hydride Transfer by La ³⁺ Cations in Zeolites during Acid Catalyzed Alkane Reactions. ACS Catalysis, 2014, 4, 1743-1752.	11.2	46
46	Pore Curvature Effect on the Stability of Coâ^'MCM-41 and the Formation of Size-Controllable Subnanometer Co Clustersâ€. Journal of Physical Chemistry B, 2005, 109, 2285-2294.	2.6	45
47	Synthesis and Characterization of Alkali-free, Ga-Substituted MCM-41 and Its Performance for n-Hexane Conversion. Journal of Catalysis, 1998, 175, 1-6.	6.2	40
48	Reversible coordination change of chromium in Cr-MCM-41 and Cr-MCM-48 studied by X-ray absorption near edge structure. Microporous and Mesoporous Materials, 2001, 48, 165-170.	4.4	40
49	Effect of Co-MCM-41 Conversion to Cobalt Silicate for Catalytic Growth of Single Wall Carbon Nanotubes. Journal of Physical Chemistry B, 2004, 108, 20095-20101.	2.6	40
50	Characterization of multi-walled carbon nanotubes catalyst supports by point of zero charge. Catalysis Today, 2011, 164, 68-73.	4.4	40
51	Promotion of protolytic pentane conversion on H-MFI zeolite by proximity of extra-framework aluminum oxide and BrAֻnsted acid sites. Journal of Catalysis, 2019, 370, 424-433.	6.2	40
52	Fundamental Role of Oxygen Stoichiometry in Controlling the Band Gap and Reactivity of Cupric Oxide Nanosheets. Journal of the American Chemical Society, 2016, 138, 10978-10985.	13.7	39
53	CoSO4/SiO2 catalyst for selective synthesis of (9, 8) single-walled carbon nanotubes: Effect of catalyst calcination. Journal of Catalysis, 2013, 300, 91-101.	6.2	38
54	Time-resolved infrared emission studies of CO2 formed by CO oxidation on Pt and Pd. Chemical Physics Letters, 1983, 102, 37-40.	2.6	37

#	Article	lF	CITATIONS
55	Characterization of Pt/L-zeolite catalysts by chemisorption, EXAFS and reaction of neopentane with H2. Catalysis Today, 1992, 15, 431-442.	4.4	37
56	Comparing characterization of functionalized multi-walled carbon nanotubes by potentiometric proton titration, NEXAFS, and XPS. Chinese Journal of Catalysis, 2014, 35, 856-863.	14.0	37
57	Adsorption of Multimeric T Cell Antigens on Carbon Nanotubes: Effect on Protein Structure and Antigenâ€&pecific T Cell Stimulation. Small, 2013, 9, 666-672.	10.0	36
58	Nitrogen Modified Carbon Nano-Materials as Stable Catalysts for Phosgene Synthesis. ACS Catalysis, 2016, 6, 5843-5855.	11.2	36
59	Multivariate correlation and prediction of the synthesis of vanadium substituted mesoporous molecular sieves. Microporous and Mesoporous Materials, 2004, 67, 245-257.	4.4	35
60	Statistical design and modeling of the process of methane partial oxidation using V-MCM-41 catalysts and the prediction of the formaldehyde production. Applied Catalysis A: General, 2006, 313, 1-13.	4.3	35
61	Ptâ^'Co Bimetallic Catalyst Supported on Single-Walled Carbon Nanotubes: Effect of Alloy Formation and Oxygen Containing Groups. Journal of Physical Chemistry C, 2010, 114, 16996-17002.	3.1	34
62	The effect of synthesis solution pH on the physicochemical properties of Co substituted MCM-41. Topics in Catalysis, 2005, 34, 31-40.	2.8	33
63	Synthesis and Characterization of Nanocomposites with Strong Interfacial Interaction: Sulfated ZrO ₂ Nanoparticles Supported on Multiwalled Carbon Nanotubes. Journal of Physical Chemistry C, 2012, 116, 21742-21752.	3.1	33
64	Photoluminescence Study of the Introduction of V in Si-MCM-41:Â Role of Surface Defects and Their Associated SiO-and SiOH Groups. Journal of Physical Chemistry B, 2003, 107, 3856-3861.	2.6	32
65	High-Yield Hydrogen Production from Aqueous Phase Reforming over Single-Walled Carbon Nanotube Supported Catalysts. ACS Catalysis, 2012, 2, 1480-1486.	11.2	31
66	Role of Spatial Constraints of BrÃ,nsted Acid Sites for Adsorption and Surface Reactions of Linear Pentenes. Journal of the American Chemical Society, 2017, 139, 8646-8652.	13.7	31
67	Importance of Methane Chemical Potential for Its Conversion to Methanol on Cuâ€Exchanged Mordenite. Chemistry - A European Journal, 2020, 26, 7563-7567.	3.3	31
68	Tailoring silica–alumina-supported Pt–Pd as poison-tolerant catalyst for aromatics hydrogenation. Journal of Catalysis, 2013, 304, 135-148.	6.2	31
69	Radius of curvature effect of V-MCM-41 probed by methanol oxidation. Journal of Catalysis, 2005, 234, 318-327.	6.2	30
70	Bimetallic Pt–Pd/silica–alumina hydrotreating catalysts. Part II: Structure–activity correlations in the hydrogenation of tetralin in the presence of dibenzothiophene and quinoline. Journal of Catalysis, 2012, 292, 13-25.	6.2	29
71	Surfactant chain length effect on the hexagonal-to-cubic phase transition in mesoporous silica synthesis. Microporous and Mesoporous Materials, 2012, 147, 242-251.	4.4	29
72	Time-Resolved Infrared Emission Studies of CO2Formed by Catalytic Oxidation of CO on Pt and Pd Surfaces. Bulletin of the Chemical Society of Japan, 1992, 65, 2450-2455.	3.2	28

#	Article	IF	CITATIONS
73	Hydrothermal synthesis of MCM-41 using different ratios of colloidal and soluble silica. Microporous and Mesoporous Materials, 2005, 81, 191-200.	4.4	28
74	Structure sensitivity of hydrogenolytic cleavage of endocyclic and exocyclic C–C bonds in methylcyclohexane over supported iridium particles. Journal of Catalysis, 2013, 297, 70-78.	6.2	28
75	Support effects on selectivity over rhodium bimetallic catalysts. Faraday Discussions of the Chemical Society, 1981, 72, 109.	2.2	27
76	Improved synthesis of highly ordered Co-MCM-41. Microporous and Mesoporous Materials, 2007, 101, 200-206.	4.4	27
77	High-Yield Single-Walled Carbon Nanotubes Synthesized on the Small-Pore (C10) Co-MCM-41 Catalyst. Journal of Physical Chemistry C, 2008, 112, 12442-12454.	3.1	27
78	Effect of chromium addition to the Co-MCM-41 catalyst in the synthesis of single wall carbon nanotubes. Applied Catalysis A: General, 2009, 368, 40-49.	4.3	27
79	Desorption of carbon dioxide molecules from a Pt(111) surface: A stochastic classical trajectory approach. Chemical Physics Letters, 1988, 144, 533-540.	2.6	26
80	A comparison of the dynamics of CO oxidation by oxygen atoms and molecules on Pt and Pd surfaces. Journal of Chemical Physics, 1996, 105, 810-824.	3.0	26
81	Single-wall carbon nanotube synthesis by CO disproportionation on nickel-incorporated MCM-41. Nanotechnology, 2005, 16, S476-S483.	2.6	26
82	Active sites and reactive intermediates in the hydrogenolytic cleavage of C–C bonds in cyclohexane over supported iridium. Journal of Catalysis, 2012, 295, 133-145.	6.2	26
83	A novel synthesis route for bimetallic CoCr–MCM-41 catalysts with higher metal loadings. Their application in the high yield, selective synthesis of Single-Wall Carbon Nanotubes. Journal of Catalysis, 2010, 271, 358-369.	6.2	25
84	Bimetallic Pt–Pd/silica–alumina hydrotreating catalysts – Part I: Physicochemical characterization. Journal of Catalysis, 2012, 292, 1-12.	6.2	25
85	Characterization of functional groups on oxidized multi-wall carbon nanotubes by potentiometric titration. Catalysis Today, 2015, 249, 23-29.	4.4	25
86	Internal reflection spectroscopy of adsorbed molecules on metal films: Carbon monoxide on palladium. Journal of Catalysis, 1975, 40, 249-254.	6.2	24
87	An X-Ray Absorption Spectroscopy Determination of the Morphology of Palladium Particles in K L-Zeolite. Journal of Catalysis, 1997, 166, 75-88.	6.2	24
88	Effect of different carbon sources on the growth of single-walled carbon nanotube from MCM-41 containing nickel. Carbon, 2007, 45, 2217-2228.	10.3	23
89	X-ray Absorption Spectroscopic Investigation of Partially Reduced Cobalt Species in Coâ^'MCM-41 Catalysts during Synthesis of Single-Wall Carbon Nanotubes. Journal of Physical Chemistry B, 2005, 109, 16332-16339.	2.6	22
90	Impact of the Local Concentration of Hydronium Ions at Tungstate Surfaces for Acid-Catalyzed Alcohol Dehydration. Journal of the American Chemical Society, 2021, 143, 20133-20143.	13.7	20

#	Article	IF	CITATIONS
91	Gas-adsorbate collisional effects and surface diffusion in porous materials. AICHE Journal, 1980, 26, 355-363.	3.6	19
92	Catalytic Consequences of Particle Size and Chloride Promotion in the Ring-Opening of Cyclopentane on Pt/Al ₂ O ₃ . ACS Catalysis, 2013, 3, 328-338.	11.2	19
93	Increase in the yield of (and selective synthesis of large-diameter) single-walled carbon nanotubes through water-assisted ethanol pyrolysis. Journal of Catalysis, 2014, 309, 419-427.	6.2	19
94	Hydration effects of Al2(MoO4)3 and AlPO4 phases in hydrotreating catalysts studied by solid state nuclear magnetic resonance spectroscopy. Catalysis Letters, 1992, 14, 1-9.	2.6	18
95	Fabrication of Discrete Nanosized Cobalt Particles Encapsulated Inside Single-Walled Carbon Nanotubes. Journal of Physical Chemistry C, 2010, 114, 11092-11097.	3.1	18
96	Mechanism for strong binding of CdSe quantum dots to multiwall carbon nanotubes for solar energy harvesting. Nanoscale, 2013, 5, 6893.	5.6	18
97	Solid-state nuclear magnetic resonance spectroscopic investigation of hydrotreating catalysts and related materials. Applied Catalysis A: General, 1993, 98, 195-210.	4.3	17
98	Controlling the Particle Size of ZrO ₂ Nanoparticles in Hydrothermally Stable ZrO ₂ /MWCNT Composites. Langmuir, 2012, 28, 17159-17167.	3.5	17
99	Direct measurement of vibrational level populations in CO2 produced during CO oxidation on Pd. Journal of Chemical Physics, 1990, 92, 5752-5754.	3.0	16
100	Application of the Generalized 2D Correlation Analysis to Dynamic Near-Edge X-ray Absorption Spectroscopy Data. Journal of the American Chemical Society, 2005, 127, 1906-1912.	13.7	16
101	Rate enhancement of phenol hydrogenation on Pt by hydronium ions in the aqueous phase. Journal of Catalysis, 2021, 404, 579-593.	6.2	16
102	Statistical analysis of synthesis of Co-MCM-41 catalysts for production of aligned single walled carbon nanotubes (SWNT). Microporous and Mesoporous Materials, 2004, 74, 133-141.	4.4	15
103	Controlled cutting of single-walled carbon nanotubes and low temperature annealing. Carbon, 2013, 63, 61-70.	10.3	15
104	Indirect effect of the strong metal-support interaction on the metal-metal inter-action in Rh-Ag/TiO2 catalysts. Applied Catalysis, 1983, 8, 99-107.	0.8	14
105	Adsorption characterization of mesoporous molecular sieves. Studies in Surface Science and Catalysis, 1998, 117, 77-84.	1.5	14
106	Effect of reaction temperature in the selective synthesis of single wall carbon nanotubes (SWNT) on a bimetallic CoCr-MCM-41 catalyst. Applied Catalysis A: General, 2010, 374, 213-220.	4.3	14
107	Surface diffusion of stearic acid on aluminum oxide. AICHE Journal, 1974, 20, 735-742.	3.6	13
108	Controlling of Physicochemical Properties of Nickel-Substituted MCM-41 by Adjustment of the Synthesis Solution pH and Tetramethylammonium Silicate Concentration. Journal of Physical Chemistry B, 2006, 110, 5927-5935.	2.6	13

#	Article	IF	CITATIONS
109	Clarifying the multiple roles of confinement in zeolites: From stabilization of transition states to modification of internal diffusion rates. Journal of Catalysis, 2019, 372, 382-387.	6.2	13
110	On the deactivation of Pt/L-zeolite catalysts. Catalysis Letters, 1993, 17, 127-137.	2.6	12
111	The effect of water on the infrared spectra of CO adsorbed on Pt/K L-zeolite. Catalysis Letters, 1997, 44, 135-144.	2.6	12
112	Pseudomorphic Synthesis of Large-Particle Coâ^'MCM-41. Chemistry of Materials, 2006, 18, 5584-5590.	6.7	12
113	Neopentane Conversion over Zeolite-Supported Platinum and Palladium Catalysts. Journal of Catalysis, 1997, 167, 425-437.	6.2	11
114	Statistical design of C10-Co-MCM-41 catalytic template for synthesizing smaller-diameter single-wall carbon nanotubes. Microporous and Mesoporous Materials, 2005, 86, 303-313.	4.4	11
115	Metal nanoparticles inside multi-walled carbon nanotubes: A simple method of preparation and of microscopic image analysis. Microporous and Mesoporous Materials, 2013, 176, 139-144.	4.4	11
116	Hydrogenation of tetralin over Pt catalysts supported on sulfated zirconia and amorphous silica alumina. Catalysis Science and Technology, 2013, 3, 2365.	4.1	10
117	H-Transfer reactions of internal alkenes with tertiary amines as H-donors on carbon supported noble metals. Organic and Biomolecular Chemistry, 2018, 16, 1172-1177.	2.8	10
118	Titanium containing MCM-41 molecular sieves prepared by secondary treatment. Studies in Surface Science and Catalysis, 1998, 117, 191-200.	1.5	9
119	New Approach to Avoid Erroneous Interpretation of Results Derived from Generalized Two-Dimensional Correlation Analysis for Applications in Catalysis. Applied Spectroscopy, 2005, 59, 1060-1067.	2.2	9
120	Rate Enhancement of Acid-Catalyzed Alcohol Dehydration by Supramolecular Organic Capsules. ACS Catalysis, 2020, 10, 13371-13376.	11.2	9
121	Spectroscopic analysis of local structure and small particles of catalysts. Applications of Surface Science, 1985, 20, 351-381.	1.0	8
122	The study of translational excitation of CO2 produced from CO oxidation on Pd using high resolution infrared chemiluminescence spectroscopy. Journal of Chemical Physics, 1995, 103, 6806-6810.	3.0	8
123	High-Temperature Stability of Cobalt Grafted on Low-Loading Incorporated Moâ ^{~,} MCM-41 Catalyst for Synthesis of Single-Walled Carbon Nanotubes. Journal of Physical Chemistry C, 2011, 115, 1014-1024.	3.1	8
124	One-step synthesis of a Pt–Co–SWCNT hybrid material from a Pt–Co–MCM-41 catalyst. Journal of Materials Chemistry, 2012, 22, 25083.	6.7	8
125	Combined Zr and S XANES Analysis on S–ZrO2/MWCNT Solid Acid Catalyst. Topics in Catalysis, 2014, 57, 693-705.	2.8	8
126	Mechanistic Pathways for Methylcyclohexane Hydrogenolysis over Supported Ir Catalysts. Journal of Physical Chemistry C, 2014, 118, 20948-20958.	3.1	8

#	Article	IF	CITATIONS
127	Platinum-Nickel/L-zeolite Bimetallic Catalysts: Effect of Sulfur Exposure on Metal Particle Size and n-Hexane Aromatization Activity and Selectivity. Studies in Surface Science and Catalysis, 1994, 83, 321-329.	1.5	7
128	Radius of Curvature Effect on the Selective Oxidation of Cyclohexene Over Highly Ordered V-MCM-41. Catalysis Letters, 2007, 117, 25-33.	2.6	7
129	Synthesis of Uniform Diameter Boron-Based Nanostructures Using a Mesoporous Mgâ`Al ₂ O ₃ Template and Tests for Superconductivity. Journal of Physical Chemistry C, 2009, 113, 17661-17668.	3.1	7
130	Preparation of highly structured V-MCM-41 and determination of its acidic properties. Studies in Surface Science and Catalysis, 2000, 130, 3053-3058.	1.5	5
131	The Electronic Structure or Charge Delocalization of Sulfated Zirconia (Supported on Multi-walled) Tj ETQq1 1 C 774-784.).784314 rg 2.8	gBT /Overloc 5
132	Chapter 3 Catalyst characterization: structure/function. Catalysis Today, 1994, 22, 261-280.	4.4	4
133	Selective Heterogeneous Transfer Hydrogenation from Tertiary Amines to Alkynes. ACS Catalysis, 2021, 11, 5405-5415.	11.2	4
134	A Diamond Internal Reflection Cell for Infrared Measurements on Metal and Metal Oxide Films. Applied Spectroscopy, 1990, 44, 159-162.	2.2	3
135	Magnetic study of the Co-MCM-41 catalyst: Before and after reaction. Journal of Applied Physics, 2011, 110, 103904.	2.5	3
136	Importance of Methane Chemical Potential for Its Conversion to Methanol on Cuâ€exchanged Mordenite. Chemistry - A European Journal, 2020, 26, 7515-7515.	3.3	3
137	Formation of Size Controllable Sub-nanometer Metallic Clusters by Pore Radius of Curvature Effect and the Stability Explained by Anchoring/Occlusion Effect. Studies in Surface Science and Catalysis, 2007, 172, 321-324.	1.5	2
138	Templated one-step catalytic fabrication of uniform diameter MgxBy nanostructures. Journal of Materials Chemistry C, 2013, 1, 2568.	5.5	2
139	The Mechanism of Olefin Isomerization on Different Forms of Chromia Investigated by Microwave Spectroscopy. Studies in Surface Science and Catalysis, 1981, 7, 965-977.	1.5	1
140	Methoxy formation/spillover on Pd/Al2O3 studied by 13C, 1H NMR. Studies in Surface Science and Catalysis, 1993, 77, 223-228.	1.5	0
141	Study of chromium species in the Cr-MCM-48 mesoporous materials by Raman spectroscopy. Studies in Surface Science and Catalysis, 2003, 146, 371-374.	1.5	0
142	Reply to the Comment on "Photoluminescence Study of the Introduction of V in Si-MCM-41:  Role of Surface Defects and Their Associated SiO- and SiOH Groups― Journal of Physical Chemistry B, 2004, 108, 5151-5152.	2.6	0
143	Synthesis, Characterizations, and Applications of Metal-Ions Incorporated High Quality MCM-41 Catalysts. Korean Chemical Engineering Research, 2013, 51, 443-454.	0.2	0